Investigating Sodium Storage Mechanisms in Tin Anodes: A Combined Pair Distribution Function Analysis, Density Functional Theory, and Solid-State NMR Approach

Joshua M. Stratford,[†] Martin Mayo,[‡] Phoebe K. Allan,[†,§,‖] Oliver Pecher,[†] Olaf J. Borkiewicz,[⊥] Kamila M. Wiaderek,[⊥] Karena W. Chapman,[⊥] Chris J. Pickard,[#,▽] Andrew J. Morris,[*,‡,□] and Clare P. Grey[*,†]

[†] Department of Chemistry, University of Cambridge, Lensfield Road, Cambridge CB2 1EW, U.K.
[‡] Cavendish Laboratory, University of Cambridge, J. J. Thomson Avenue, Cambridge CB3 0HE, U.K.
[§] Gonville and Caius College, Trinity Street, Cambridge CB2 1TA, U.K.
[‖] Diamond Light Source Ltd., Harwell Science and Innovation Campus, Didcot OX11 0DE, U.K.
[⊥] X-ray Science Division, Advanced Photon Source, Argonne National Laboratory, Argonne, Illinois 60439, United States
[#] Department of Materials Science and Metallurgy, 27 Charles Babbage Road, Cambridge CB3 0FS, U.K.
[▽] Advanced Institute for Materials Research, Tohoku University, 2-1-1 Katahira, Aoba-ku, Sendai 980-8577, Japan
[□] Department of Physics, University of Warwick, Gibbet Hill Road, Coventry CV4 7AL, U.K.

* Corresponding authors:
Professor Clare P. Grey, email: cpg27@cam.ac.uk
Dr Andrew J. Morris, email: ajm255@cam.ac.uk

Supplementary Information

Description of the experimental and predicted Na_xSn phases found within 0.02 eV/atom of the convex hull

Table S1. Description of the experimental and predicted Na_xSn phases found within 0.02 eV/atom of the convex hull. We indicate with a star (⋆) the stable phases which are found on the convex hull.

Stoichometry	x in Na_xSn	Distance from the hull [eV/atom]	Space group	Structure origin
Sn ⋆	0	0	$I4_1/amd$	
$NaSn_{17}$	0.059	0.018	$Fd\bar{3}m$	Swap from $Na_{0.40}Si_{17}$ [1]†
$NaSn_5$ ⋆	0.2	0	$P\bar{4}2_1m$	Known Na-Sn phase[2]
$NaSn_4$	0.25	0.011	Cc	AIRSS structure
$NaSn_3$	0.333	0.007	$Pmmm$	Derived from $NaSn_2$-$P6/mmm$
		0.012	$Pm\bar{3}m$	AIRSS structure
$NaSn_2$ ⋆	0.5	0	$P6/mmm$	AIRSS structure
Na_5Sn_8 ⋆	0.625	0	$P2/c$	Known Na-Sn phase $Na_{1.17}Sn_2$ [3] †
NaSn ⋆	1	0	$I4_1/acd$	Known Na-Sn phase[4]
Na_2Sn	2	0.01	$P2_1/c$	AIRSS structure
		0.02	$R\bar{3}m$	Swap from Li_2Si [5]
Na_9Sn_4	2.25	0.004	$P6_3/mmc$	Known Na-Sn phase[6]
Na_7Sn_3 ⋆	2.333	0	$P3_212$	Swap from Li_7Si_3 [7]
Na_5Sn_2	2.5	0.006	$R\bar{3}m$	Swap from Li_5Sn_2 [8]
$Na_{13}Sn_5$	2.6	0.005	$P\bar{3}m1$	Swap from $Li_{13}Sn_5$ [9]
Na_8Sn_3	2.667	0.006	$R\bar{3}m$	Swap from Li_8Pb_3 [10]
$Na_{13}Sn_4$	3.25	0.007	$Pbam$	Swap from $Li_{13}Si_4$ [11]
$Na_{15}Sn_4$ ⋆	3.75	0	$I\bar{4}3d$	Known Na-Sn phase[12]
Na_4Sn	4	0.006	$Pnma$	Known Na-Sn phase $Na_{14.8}Sn_4$ [12] †
$Na_{21}Sn_5$	4.2	0.01	$F\bar{4}3m$	Swap from $Li_{21}Si_5$ [7]
$Na_{17}Sn_4$	4.25	0.011	$F\bar{4}3m$	Swap from $Li1_7Sn_4$ [13]
Na ⋆		0	$Im\bar{3}m$	

† Partial occupancies were set to one.

Electrochemistry plotted as a function of capacity

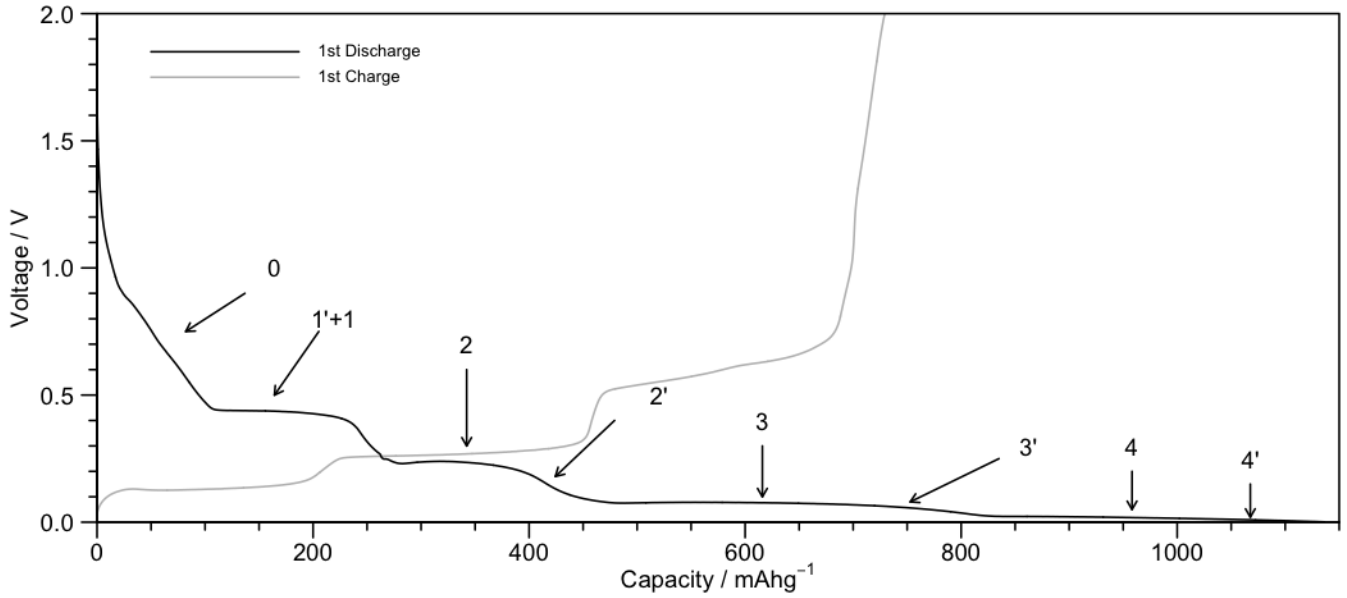

Figure S1. Electrochemistry data for a sodium-tin cell cycled at a rate of C/20 (corresponding to achieving a capacity of 847 mAhg^{-1} in 20 hours) between 2 and 0.001 V (black line). The first discharge is plotted as a black line, the first charge in grey.

***Operando* X-ray diffraction measurements during electrochemical process 0**

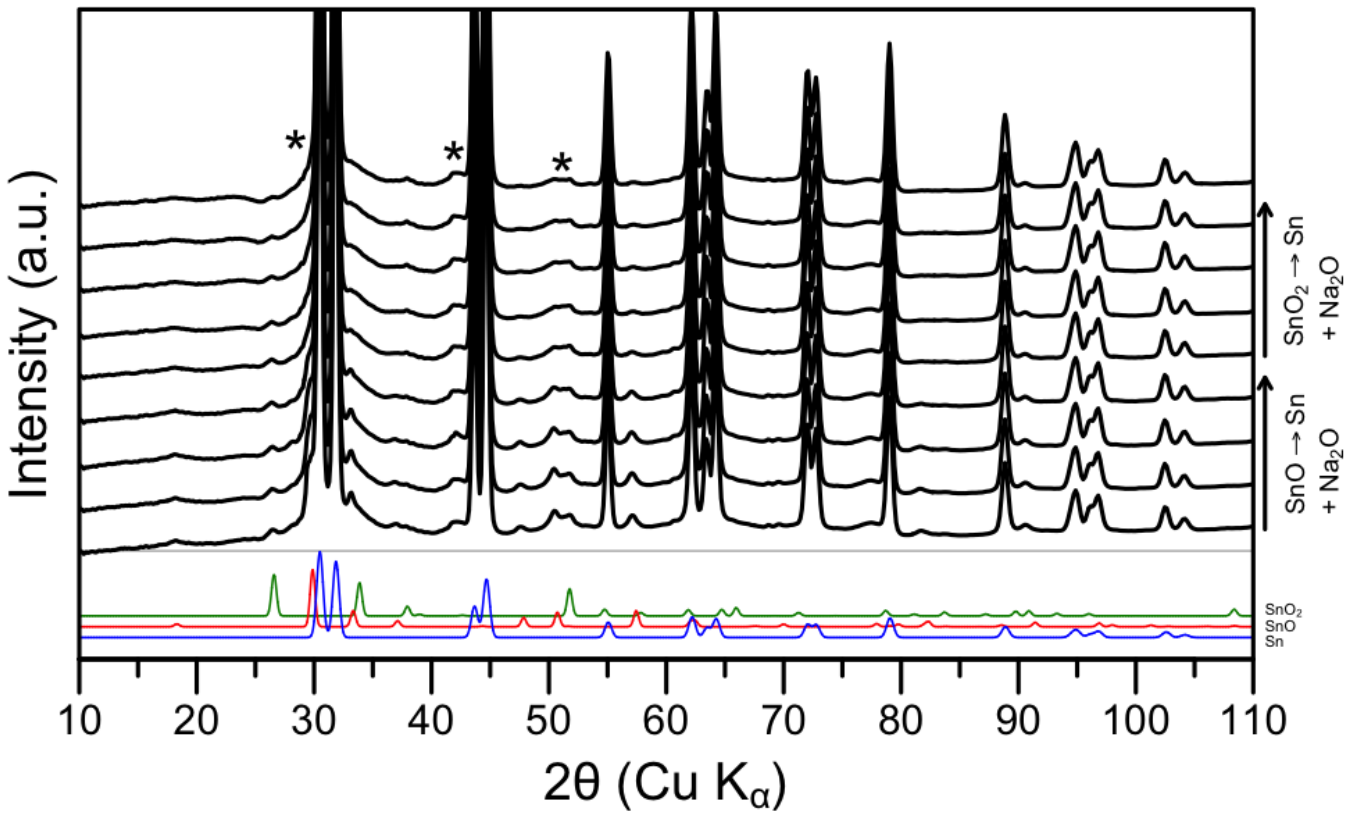

Figure S2. Diffraction patterns obtained during an *operando* experiment from the start of discharge until the end of the electrochemical process 0. Calculated patterns are shown for Sn (blue), SnO (red) and SnO_2 (green). Trace amounts of sodium from the cell background are indicated with an asterisk (*). The cell was cycled at a rate of C/70 (corresponding to achieving the theoretical capacity in 70 hours) and data were gathered at 2 hour intervals. Data were gathered using X-rays of wavelength 0.1430 Å and converted to Cu K_α (1.54 Å).

***Operando* X-ray diffraction measurements during electrochemical processes 1 and 1′**

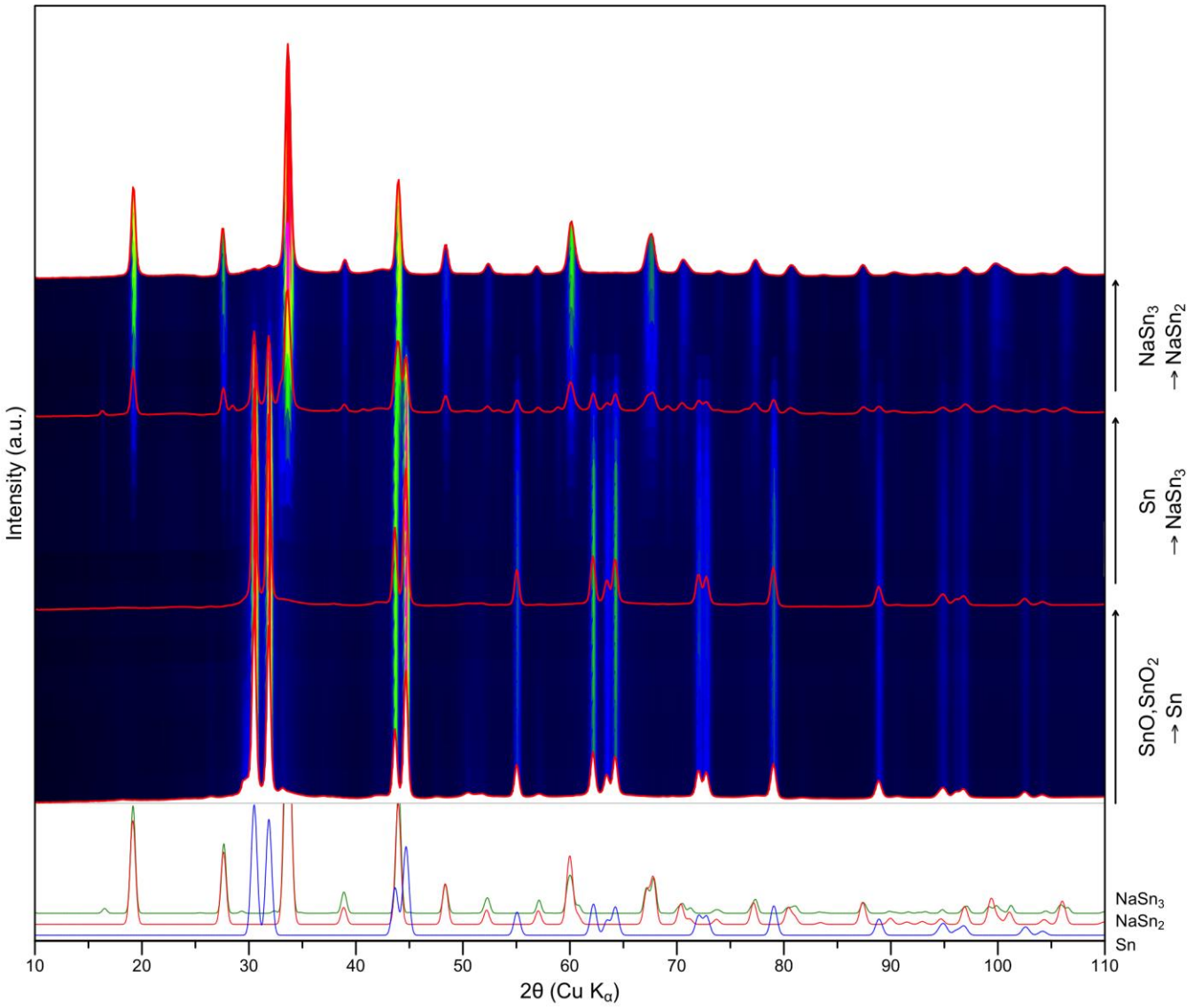

Figure S3. Diffraction patterns obtained during an *operando* experiment from the start of discharge until the end of the electrochemical processes 1 and 1′. Key frames are highlighted by solid red lines. Calculated patterns are shown for Sn (blue), $NaSn_3$ (green) and $NaSn_2$ (red). The cell was cycled at a rate of C/70 (corresponding to achieving the theoretical capacity in 70 hours) and data were gathered at 2 hour intervals. Data were gathered using X-rays of wavelength 0.1430 Å and converted to Cu K_α (1.54 Å).

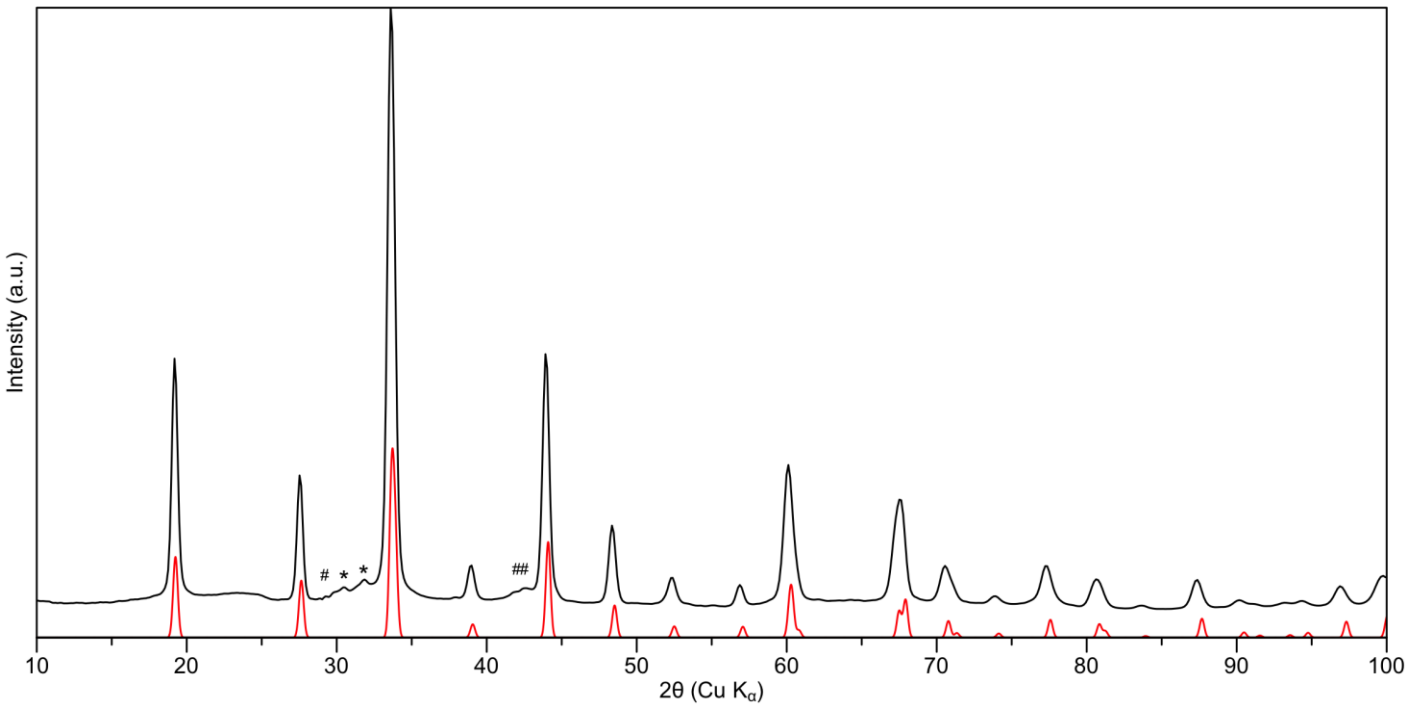

Figure S4. A conventional powder pattern showing the intermediate formed at the end of process 1′ on discharge along with the calculated pattern for $NaSn_2$ (red). Trace amounts of Na and Sn are indicated by # and * respectively. Data were gathered using X-rays of wavelength 0.1430 Å and converted to Cu K_α (1.54 Å).

Refinements of *operando* PDF data obtained during electrochemical processes 1 and 1′

The structural similarity of the two structures formed during electrochemical processes 1 and 1′ can be demonstrated by fitting the intermediate PDFs using a combination of only β-Sn (the initial structure) and $NaSn_2$ (the final structure). In all cases a R_w of less than 0.20 indicates a good match to the experimental data. This means that the intermediate formed during process 1′ must be very structurally similar to either β-Sn or $NaSn_2$. The change in the lattice parameters for $NaSn_2$ during process 1 (after approximately 150 $mAhg^{-1}$) is due to the conversion from $NaSn_3$ to $NaSn_2$. $NaSn_3$ is not included in the model, however, the relatively high values of U_{33} for Sn towards the start of these processes are consistent with tin not solely being confined to planar layers.

Real-space least-squares refinements against PDF data were performed in PDFGui.[14] A starting model of either β-Sn or $NaSn_2$ was used. Thermal displacement parameters, U, for all atoms were set to an initial value of 0.01. Unit cell parameters, phase scale factor, delta1 (low-*r* peak sharpening parameter) and the thermal parameters for both Na and Sn were all refined. For $NaSn_2$, U_{33} was refined independently of U_{11} and U_{22} (which were constrained to be the same). Qdamp (instrument resolution parameter) was set to the value obtained from a refinement of the pristine material.

Table S2. Refined parameter values determined by performing real-space least-squares refinements in PDFGui.

	Sn			$NaSn_2$						
Capacity / $mAhg^{-1}$	a / Å	c / Å	U	a / Å	c / Å	U_{Na}	$U_{33,Na}$	U_{Sn}	$U_{33,Sn}$	R_W
6.00	5.838	3.186	0.027	–	–	–	–	–	–	0.153
17.6	5.839	3.187	0.027	–	–	–	–	–	–	0.144
29.6	5.838	3.187	0.027	–	–	–	–	–	–	0.137
41.3	5.838	3.186	0.027	–	–	–	–	–	–	0.129
52.9	5.838	3.186	0.027	–	–	–	–	–	–	0.128
64.9	5.838	3.187	0.027	–	–	–	–	–	–	0.127
76.5	5.838	3.187	0.027	–	–	–	–	–	–	0.139
88.6	5.838	3.187	0.027	–	–	–	–	–	–	0.129
100.2	5.837	3.186	0.028	5.342	3.182	0.010	0.010	0.020	0.035	0.130
111.8	5.837	3.186	0.029	5.346	3.186	0.009	0.025	0.017	0.025	0.139
123.9	5.838	3.186	0.028	5.350	3.182	0.105	0.003	0.035	0.186	0.141
135.5	5.838	3.186	0.028	5.343	3.192	0.090	0.047	0.031	0.099	0.154
147.1	5.838	3.186	0.029	5.333	3.203	0.056	0.054	0.025	0.082	0.171
159.1	5.838	3.185	0.031	5.328	3.208	0.047	0.054	0.022	0.064	0.177
170.8	5.838	3.183	0.034	5.324	3.211	0.043	0.055	0.020	0.057	0.169
182.8	5.836	3.184	0.021	5.320	3.213	0.054	0.075	0.020	0.060	0.150
194.4	3.839	3.186	0.029	5.316	3.217	0.040	0.056	0.018	0.055	0.122
206.1	5.838	3.186	0.027	5.315	3.220	0.051	0.077	0.019	0.058	0.129

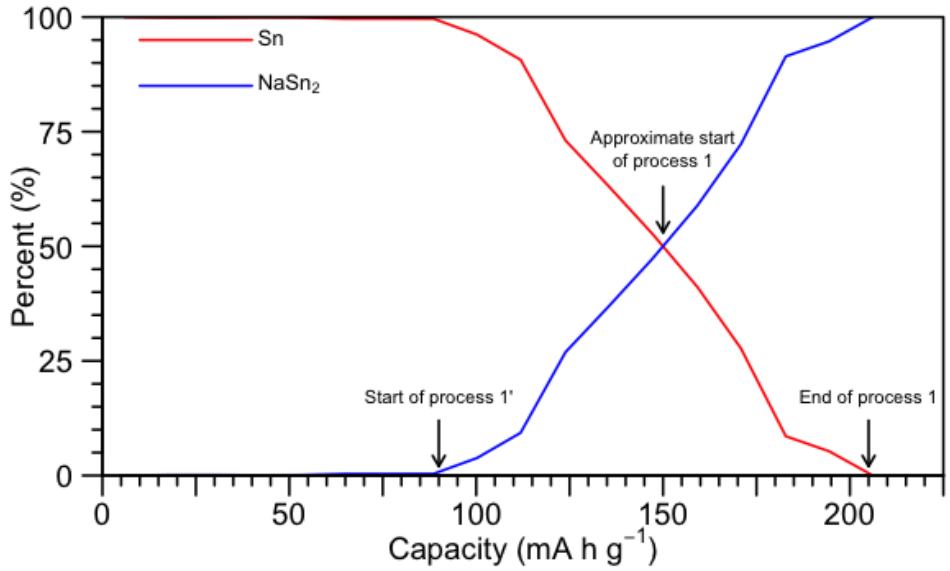

Figure S5. Proportion of Sn and $NaSn_2$ used in the PDF refinements.

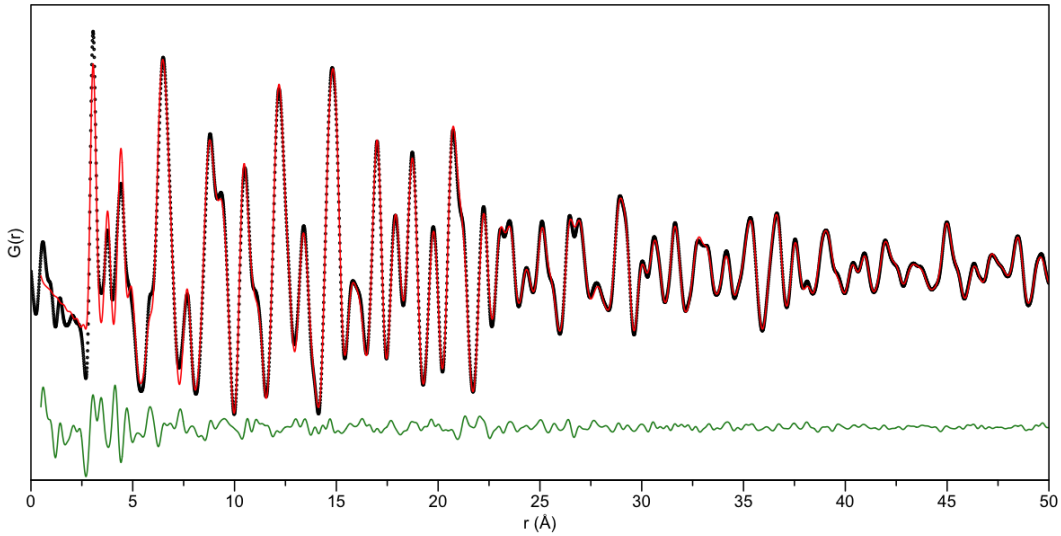

Figure S6. PDF obtained during an *operando* measurement at the end of electrochemical processes 0. Experimental data are shown as black circles, a fit to β-Sn (R_w=0.13) is shown as a red line and the difference as a green line offset below. The cell was cycled at a rate of C/70 (corresponding to achieving the theoretical capacity in 70 hours) and data were gathered at 2 hour intervals.

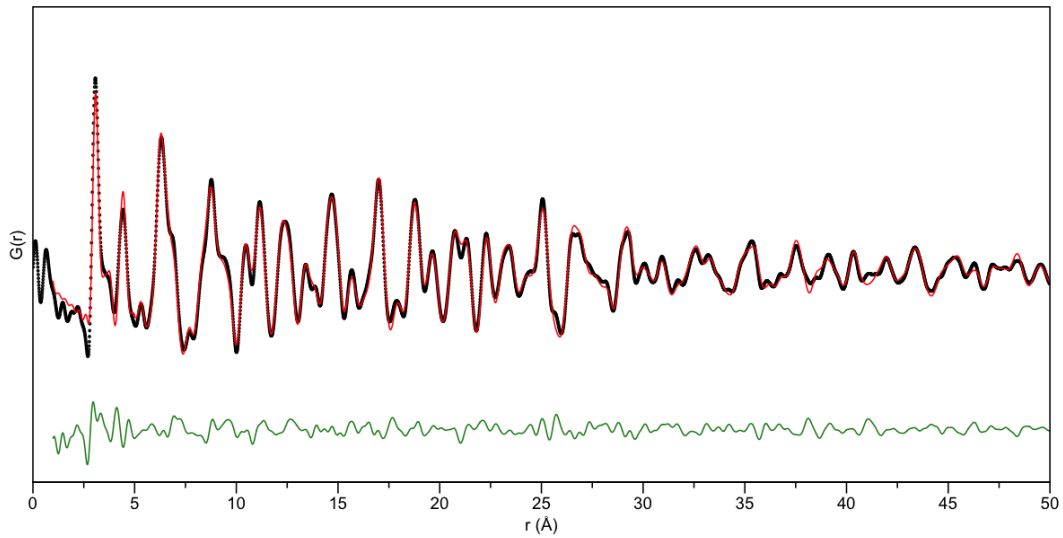

Figure S7. PDF obtained during an *operando* measurement at the end of electrochemical process 1. Experimental data are shown as black circles, a fit to a 1:1 mixture of β-Sn and $NaSn_2$ (R_w=0.18) is shown as a red line and the difference as a green line offset below. The cell was cycled at a rate of C/70 (corresponding to achieving the theoretical capacity in 70 hours) and data were gathered at 2 hour intervals.

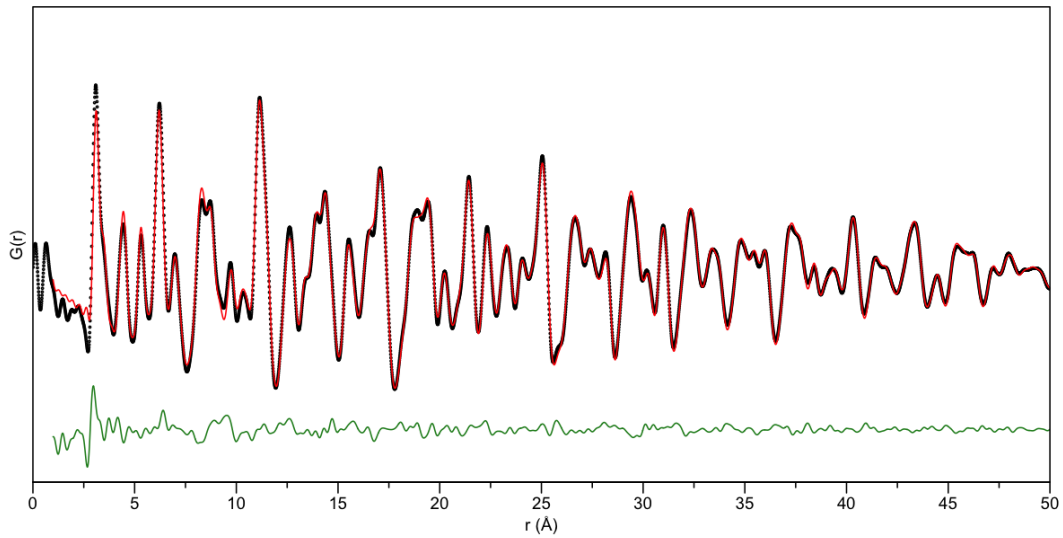

Figure S8. PDF obtained during an *operando measurement* at the end of electrochemical processes 1′. Experimental data are shown as black circles, a fit to $NaSn_2$ (R_w=0.13) is shown as a red line and the difference as a green line offset below. The cell was cycled at a rate of C/70 (corresponding to achieving the theoretical capacity in 70 hours) and data were gathered at 2 hour intervals.

Refinements of *operando* PDF data obtained during electrochemical processes 2 and 2′

Combined real- and reciprocal-space Reverse Monte-Carlo (RMC) refinements against PDF data were performed in RMCProfile.[15] We used a 10×10×10 supercell of an amorphous phase generated using *ab initio* molecular dynamics as the starting model. The minimum distance was set to 2.63 Å, which is the observed minimum distance in the experimental PDF. The number density was set to 0.0325, which is the same as the starting model. The maximum distance for an individual movement was set to 0.05 Å. The refinement was stopped when no further improvement to the fit was observed.

Following the RMC refinements, real-space least-squares refinements were performed in PDFGui.[14] As a starting model, a 61 atom subcell of the RMC refined $Na_{1.18}Sn$ was used with a spherical particle diameter of 40 Å, and $NaSn_2$ was used to account for the longer-range correlations. U_{iso} parameters for all atoms were set to an initial value of 0.01. Unit cell parameters, phase scale factor, delta1 (low-*r* peak sharpening parameter) and the thermal parameters for both Na and Sn were all refined, along with the Sn atomic positions. Qdamp (instrument resolution parameter) was set to the value obtained from a refinement of the pristine material. For $NaSn_2$, $U_{33,Sn}$ was refined independently of U_{11} and U_{22} (which were constrained to be the same), this was not possible for Na. For $Na_{1.18}Sn$ the thermal displacement parameters were considered isotropically. Results are sumarised in Table S3, note that phase fractions are not shown owing to the mixture of amorphous and crystalline components.

Table S3. Summary of the PDF refined parameters for the structures formed during electrochemical processes 2 and 2′

	$NaSn_2$					Amorphous ~$Na_{1.2}Sn$						
Capacity / $mAhg^{-1}$	a / Å	c / Å	U_{Na}	U_{Sn}	$U_{33,Sn}$	a / Å	b / Å	c / Å	Spherical Particle Diameter / Å	U_{Na}	U_{Sn}	R_W
219.632	5.308	3.226	0.057	0.027	0.026	11.65	12.49	12.218	41.196	0.014	0.007	0.165
247.17	5.308	3.226	0.057	0.027	0.026	11.65	12.49	12.218	41.196	0.014	0.007	0.137
274.248	5.307	3.227	0.057	0.029	0.026	11.621	12.57	12.237	30.155	0.013	0.009	0.16
301.786	5.304	3.231	0.057	0.023	0.028	11.584	12.584	12.205	34.253	0.018	0.013	0.224
329.323	5.292	3.233	0.057	0.027	0.065	11.615	12.591	12.229	31.818	0.019	0.014	0.246
356.86	5.23	3.572	0.057	0.059	0.284	11.612	12.446	12.276	28.629	0.024	0.015	0.265
384.398	5.197	3.618	0.129	0.071	0.241	11.709	12.437	12.269	29.058	0.014	0.024	0.273
411.476	5.197	3.618	0.129	0.071	0.241	11.709	12.437	12.269	29.058	0.014	0.024	0.26
439.013	5.2	3.614	0.129	0.06	0.191	11.709	12.437	12.269	29.058	0.014	0.024	0.255

Simulated PDF of crystalline NaSn

PDF simulations were performed in PDFGui.[14] U_{iso} parameters were set to 0.1 for Na atoms and 0.01 for Sn atoms. Delta1 (low-*r* peak sharpening parameter) was set to 1.7. Qdamp (instrument resolution parameter) was set to the value obtained from a refinement of the pristine material. An additional simulation was performed for NaSn with much greater disorder simulated using higher thermal displacement parameters – $U_{iso,Sn}$=0.05 and $U_{iso,Na}$=0.5.

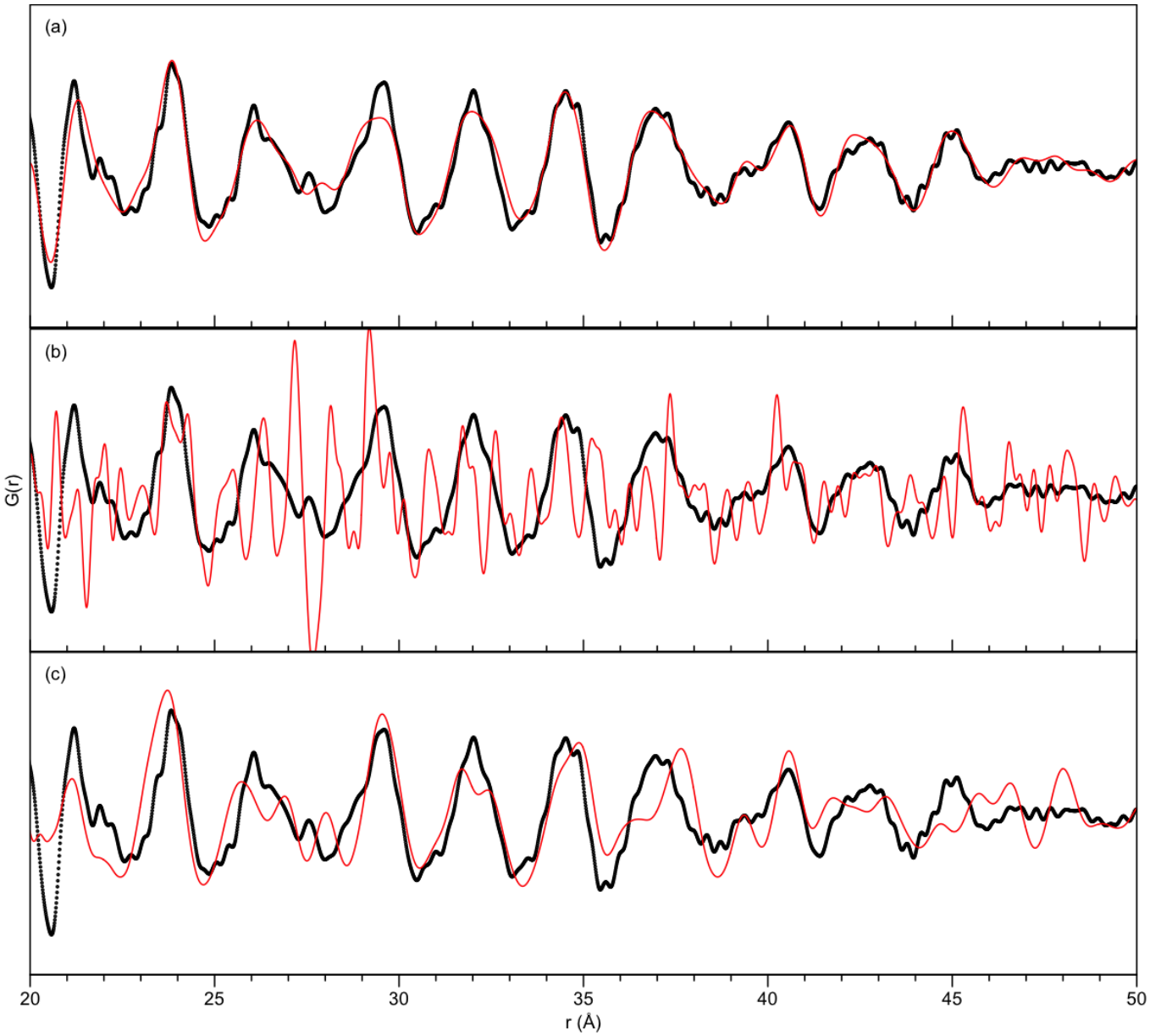

Figure S9. PDF obtained during an *operando* measurement at the end of electrochemical process 2′. Experimental data are shown as black circles, simulations of (a) expanded $NaSn_2$ (b) crystalline NaSn (c) crystalline NaSn with higher thermal displacement parameters ($U_{iso,Sn}$=0.05 and $U_{iso,Na}$=0.5) are shown as red lines.

Ex situ ^{23}Na NMR data corresponding to the structures formed during electrochemical processes 2 and 2′

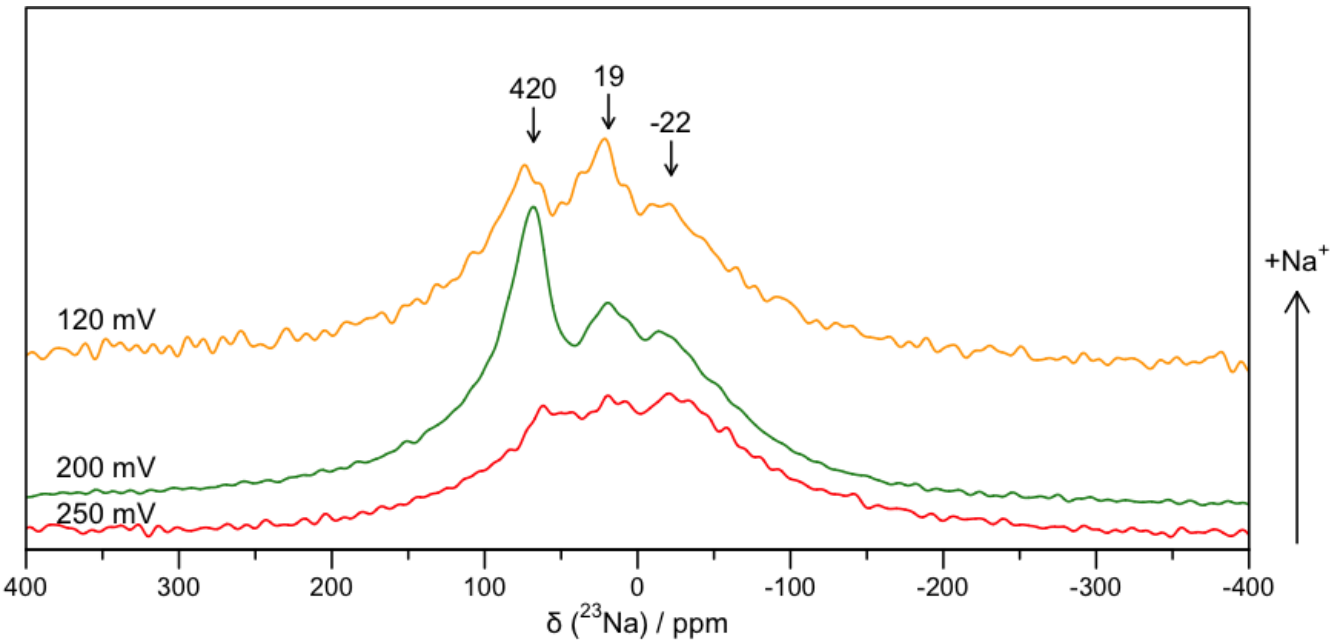

Figure S10. *Ex situ* ^{23}Na 60 kHz MAS NMR spectra of tin anodes discharged to 250 mV (bottom, red), 200 mV (middle, green) and 120 mV (top, orange). Shifts are indicated for all peak maxima. The peak with maxima around -22 ppm results from sodium within the SEI layer, carbon additive and CMC binder. Intensities have been normalised based on the sample mass and number of transients collected.

Ex situ NMR of a crystalline NaSn model compound

Tin powder (Sigma Aldrich, ≥99%, particle size ≤45 μm and sodium (Sigma Aldrich, 99.9%) in a 1:1 ratio were ball-milled under argon in a zirconia ball mill jar using a SPEX 8000M Mixer / Mill for 8 hours. The resulting powder was stored in an argon atmosphere glove box (O_2, H_2O < 0.1 ppm) prior to use. Formation of NaSn was confirmed by XRD.

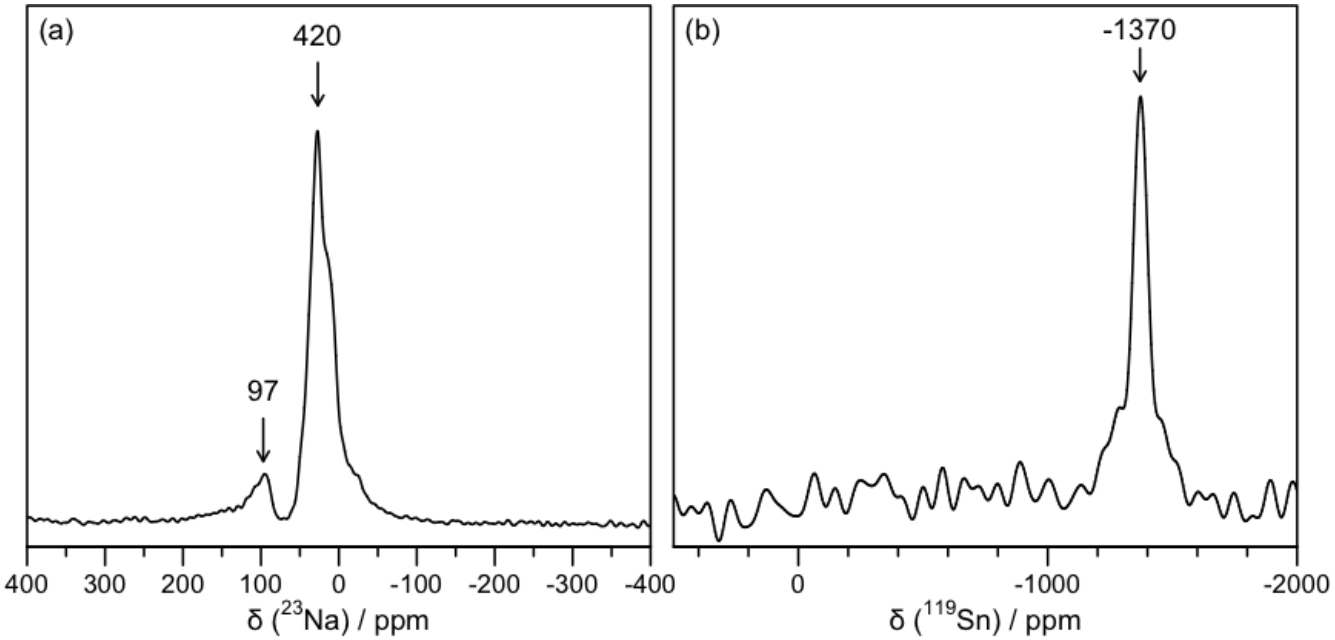

Figure S11. *Ex situ* (a) ^{23}Na (b) ^{119}Sn 60 kHz MAS NMR spectra of an NaSn model compound prepared by ball-milling. The shifts of the peak maxima are indicated.

Refinements of *operando* PDF data obtained during electrochemical processes 3 and 3′

Real-space least-squares refinements against PDF data were performed in PDFGui.[14] U_{iso} parameters for all atoms were set to an initial value of 0.01. Unit cell parameters, phase scale factor, delta1 (low-*r* peak sharpening parameter) and the thermal parameters for both Na and Sn were all refined. Qdamp (instrument resolution parameter) was set to the value obtained from a refinement of the pristine material.

Table S4. Results of preliminary real-space least-squares refinements in PDFGui for all known and predicted structures with appropriate stoichiometries for the structure formed during process 3.

Structure	Space Group	Origin	U_{Na}	U_{Sn}	R_w	
$Na_{12}Sn_7$	*Pnma*		0.004	0.034	0.38	
Na_2Sn	$P2_1/c$		0.006	0.087	0.75	
Na_2Sn	$R\bar{3}m$		0.074	0.039	0.18	*
Na_2Sn	*Cmcm*	Ref [16]	0.138	0.124	0.94	
Na_2Sn	*Cmcm*	Ref [16]	0.330	0.069	0.73	
Na_9Sn_4	*Cmcm*	Ref [6]	0.020	0.040	0.45	
Na_7Sn_3	$P2_1/m$		0.151	0.036	0.45	
Na_7Sn_3	$R\bar{3}m$	Ref [16]	0.097	0.037	0.18	*
Na_5Sn_2	$R\bar{3}m$		0.104	0.036	0.19	*
$Na_{13}Sn_5$	$P\bar{3}m1$		0.079	0.037	0.32	
Na_8Sn_3	$R\bar{3}m$		0.056	0.048	0.40	
Na_3Sn	*Immm*	Ref [16]	0.381	0.129	0.98	
Na_3Sn	*Pmnm*	Ref [16]	0.017	0.108	0.55	
Na_3Sn	*Pmnm*	Ref [16]	0.067	0.175	0.66	
$Na_{13}Sn_4$	*Pbam*		0.011	0.052	0.35	

* Selected for further study

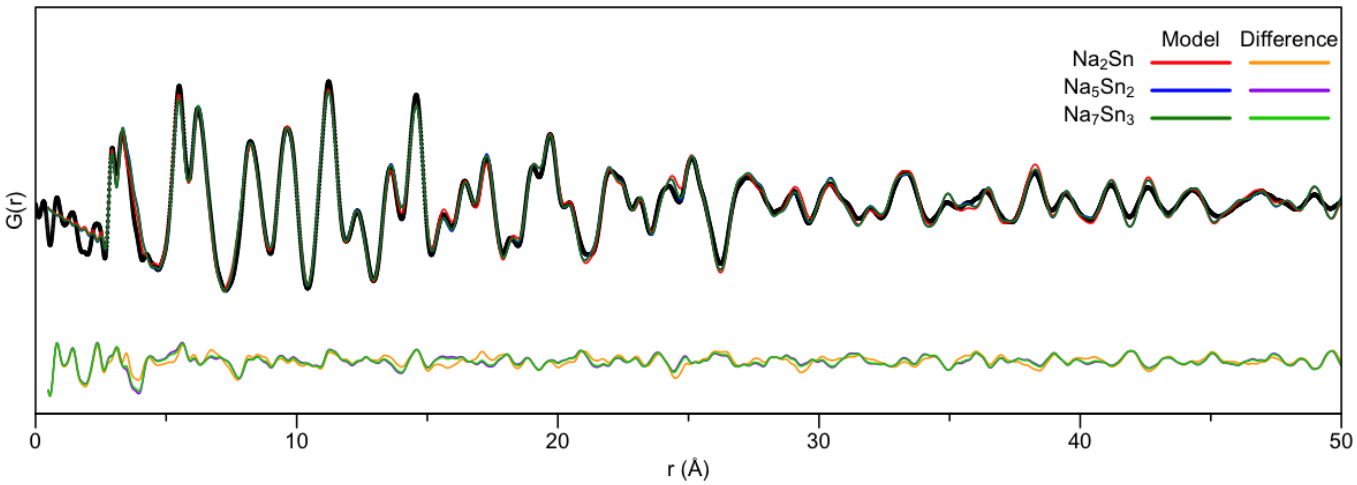

Figure S12. PDF obtained during an *operando measurement* at the end of electrochemical processes 3. Experimental data are shown as black circles, a fit to Na_2Sn is shown as a red line, Na_5Sn_2 as a blue line and Na_7Sn_3 as a green line. Differences are offset below as orange, purple and green lines, respectively.

Further real-space least-squares refinements were performed on the Na_5Sn_2 ($R\bar{3}m$) class of structures. U_{iso} parameters for all atoms were set to an initial value of 0.01. Unit cell parameters, phase scale factor, delta1 (low-*r* peak sharpening parameter) and the thermal parameters for both Na (all sites independently) and Sn were all refined. In addition, the *z*-positions of the sodium atoms were refined, and the occupancy of the Na_3 site. Qdamp (instrument resolution parameter) was set to the value obtained from a refinement of the pristine material. A range of initial values were attempted for the occupancy values, in all cases the result was the same.

Table S5. Results of real-space least-squares refinements in PDFGui for Na_5Sn_2 against *operando* PDF data obtained during electrochemical process 3′.

Capacity / $mAhg^{-1}$	a / Å	c / Å	U(Na_1)	U(Na_2)	U(Na_3)	U(Sn)	Z(Na_1)	Z(Na_2)	Z(Sn)	Occupancy (Na_3)	$Na_{15}Sn_4$ (%)	R_w
662.43	5.461	22.533	0.085	0.076	0.189	0.039	0.359	0.206	0.065	0.420	5.4	0.175
675.58	5.462	22.538	0.083	0.077	0.161	0.038	0.358	0.206	0.065	0.426	5.9	0.171
687.05	5.463	22.542	0.082	0.078	0.162	0.038	0.357	0.207	0.065	0.433	6.7	0.175
697.51	5.464	22.544	0.082	0.078	0.151	0.037	0.358	0.207	0.065	0.435	8.3	0.171
707.15	5.464	22.546	0.082	0.078	0.151	0.037	0.358	0.207	0.065	0.438	8.9	0.172
715.67	5.465	22.548	0.080	0.079	0.162	0.037	0.358	0.207	0.065	0.451	9.9	0.173
723.93	5.466	22.552	0.077	0.081	0.183	0.037	0.358	0.208	0.065	0.486	11	0.175
732.19	5.467	22.553	0.078	0.081	0.182	0.038	0.358	0.208	0.065	0.481	11.8	0.173
740.45	5.467	22.556	0.076	0.085	0.182	0.038	0.358	0.208	0.065	0.497	12.7	0.176
748.71	5.468	22.557	0.077	0.087	0.184	0.038	0.358	0.209	0.065	0.511	13.4	0.177
756.54	5.469	22.559	0.079	0.091	0.175	0.038	0.358	0.209	0.065	0.522	14.1	0.180
764.11	5.469	22.562	0.081	0.095	0.162	0.039	0.357	0.210	0.065	0.524	14.6	0.183
771.24	5.470	22.564	0.077	0.099	0.182	0.039	0.357	0.210	0.065	0.553	15.3	0.186
778.13	5.471	22.565	0.080	0.100	0.170	0.040	0.357	0.210	0.065	0.559	15.9	0.190
785.01	5.471	22.568	0.077	0.104	0.187	0.040	0.357	0.210	0.065	0.585	16.5	0.194
791.78	5.472	22.569	0.081	0.106	0.171	0.041	0.357	0.211	0.065	0.598	17.4	0.197
798.67	5.473	22.572	0.077	0.108	0.192	0.041	0.357	0.211	0.065	0.622	17.8	0.201
805.55	5.473	22.572	0.083	0.106	0.170	0.042	0.357	0.212	0.065	0.619	18.5	0.205
812.44	5.474	22.576	0.078	0.108	0.198	0.043	0.357	0.212	0.065	0.594	18.9	0.208
819.32	5.476	22.578	0.069	0.114	0.202	0.043	0.358	0.211	0.065	0.647	19.5	0.213
826.09	5.476	22.577	0.080	0.111	0.180	0.044	0.357	0.212	0.065	0.669	20.3	0.216
832.65	5.477	22.580	0.083	0.112	0.174	0.045	0.357	0.213	0.065	0.692	20.9	0.218
838.46	5.477	22.580	0.083	0.113	0.173	0.046	0.357	0.213	0.065	0.706	21.2	0.223
843.97	5.478	22.583	0.083	0.117	0.168	0.046	0.356	0.213	0.065	0.728	22	0.226
849.47	5.479	22.584	0.083	0.117	0.168	0.047	0.356	0.214	0.065	0.800	22.9	0.230
854.89	5.480	22.603	0.086	0.118	0.175	0.047	0.357	0.214	0.065	0.752	23.7	0.241
860.4	5.481	22.595	0.086	0.120	0.178	0.048	0.357	0.214	0.065	0.716	23.4	0.243
865.9	5.482	22.592	0.079	0.125	0.183	0.050	0.356	0.214	0.065	0.734	23.4	0.249
871.41	5.483	22.594	0.080	0.125	0.177	0.051	0.356	0.214	0.065	0.739	23.9	0.251
876.92	5.483	22.594	0.080	0.125	0.177	0.051	0.356	0.214	0.065	0.739	23.9	0.257
878.94	5.483	22.594	0.080	0.125	0.177	0.051	0.356	0.214	0.065	0.739	23.9	0.267

In addition to directly refining the Na(3) occupancy, the expected increase in occupancy was inferred using the unit cell volume expansion. A radius of 1.10 Å was assumed for the sodium ion, consistent with sodium having a coordination number between 6 and 8,[17] and a starting occupancy of 0.40 was also assumed based upon the refined value. The unit cell volume was calculated as $a^2c\sin\gamma$, and the expected occupancy as $\frac{1}{3}\cdot\frac{V_i-V_{i-1}}{\frac{4}{3}\pi(1.10)^3}+0.4$ where V_i is the refined volume of the unit cell for the *i*th dataset.

Table S6. Data used for the expected occupancy values shown in Figure 7

Capacity / $mAhg^{-1}$	Volume / $Å^3$	Expansion / $Å^3$	Additional Na	Expected Occupancy
662.43	581.91	0.00	0.00	0.40
675.58	582.26	0.35	0.06	0.42
687.05	582.53	0.62	0.11	0.44
697.51	582.84	0.92	0.17	0.46
707.15	582.95	1.04	0.19	0.46
715.67	583.17	1.26	0.22	0.47
723.93	583.47	1.56	0.28	0.49
732.19	583.66	1.75	0.31	0.50
740.45	583.90	1.99	0.36	0.52
748.71	584.05	2.14	0.38	0.53
756.54	584.27	2.36	0.42	0.54
764.11	584.44	2.53	0.45	0.55
771.24	584.68	2.77	0.50	0.57
778.13	584.84	2.93	0.52	0.57
785.01	585.07	3.16	0.57	0.59
791.78	585.28	3.37	0.60	0.60
798.67	585.46	3.55	0.63	0.61
805.55	585.64	3.73	0.67	0.62
812.44	585.94	4.02	0.72	0.64
819.32	586.27	4.36	0.78	0.66
826.09	586.32	4.41	0.79	0.66
832.65	586.60	4.69	0.84	0.68
838.46	586.66	4.75	0.85	0.68
843.97	586.98	5.06	0.91	0.70
849.47	587.17	5.26	0.94	0.71
854.89	587.83	5.92	1.06	0.75
860.4	587.75	5.84	1.04	0.75
865.9	587.94	6.02	1.08	0.76
871.41	588.18	6.27	1.12	0.77
876.92	588.18	6.27	1.12	0.77
878.94	588.18	6.27	1.12	0.77

Ex situ NMR data corresponding to the structures formed during electrochemical process 3

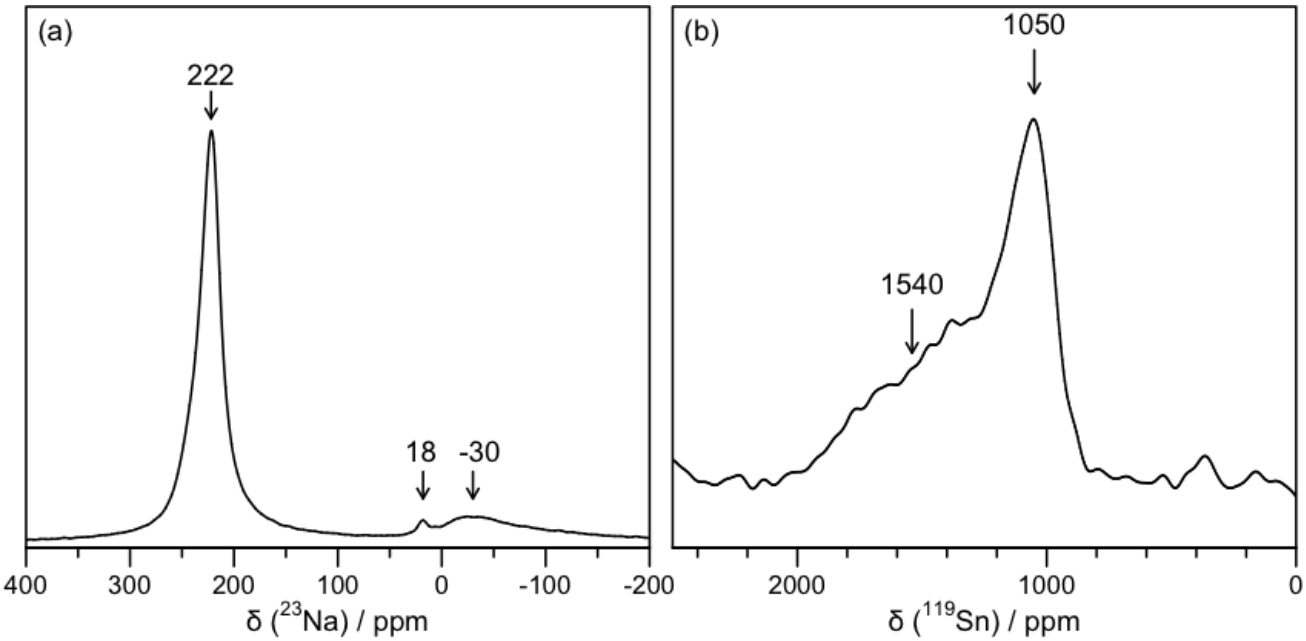

Figure S13. (a) *Ex situ* ^{23}Na 60 kHz MAS NMR spectra of a tin anode discharged to 50 mV. Shifts are indicated for all peak maxima. The peak with maximum around 18 ppm results from trace amounts of NaOH, the peak around -30 ppm results from sodium within the SEI layer, carbon additive and CMC binder. (b) *Ex situ* ^{119}Sn 60 kHz MAS NMR spectra of the same material. Shifts are indicated for peak maxima.

Simulated PDFs of various dumbbell NaSn phases

PDF simulations were performed in PDFGui.[14] U_{iso} parameters were set to 0.05 for Na atoms and 0.01 for Sn atoms. Delta1 (low-*r* peak sharpening parameter) was set to 1.7. Qdamp (instrument resolution parameter) was set to the value obtained from a refinement of the pristine material.

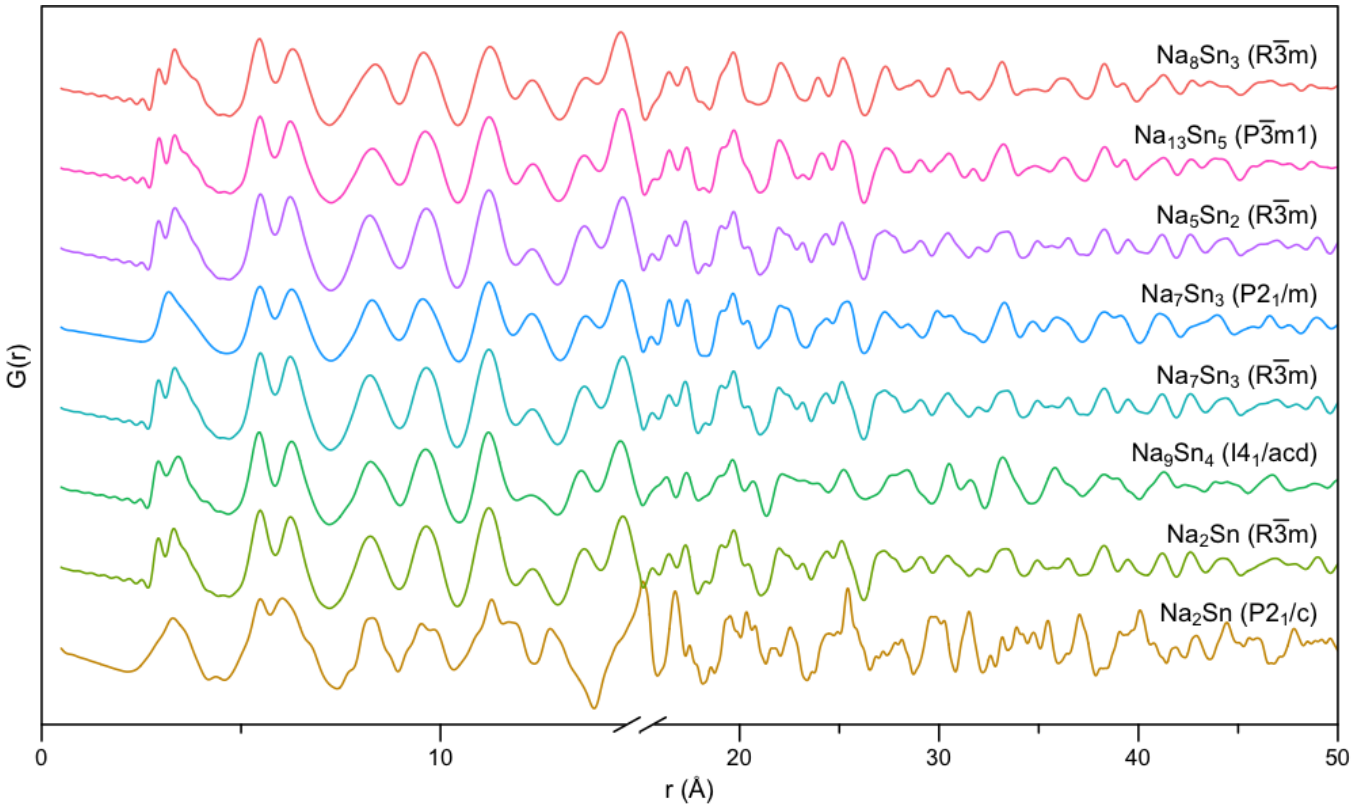

Figure S14. Simulated PDFs of several dumbbell phases. It is evident that the short-range structure of many of these structures is similar, there are, however, differences exist in the longer-range ordering.

Calculated Sn-Sn dumbbell distances for a range of dumbbell structures

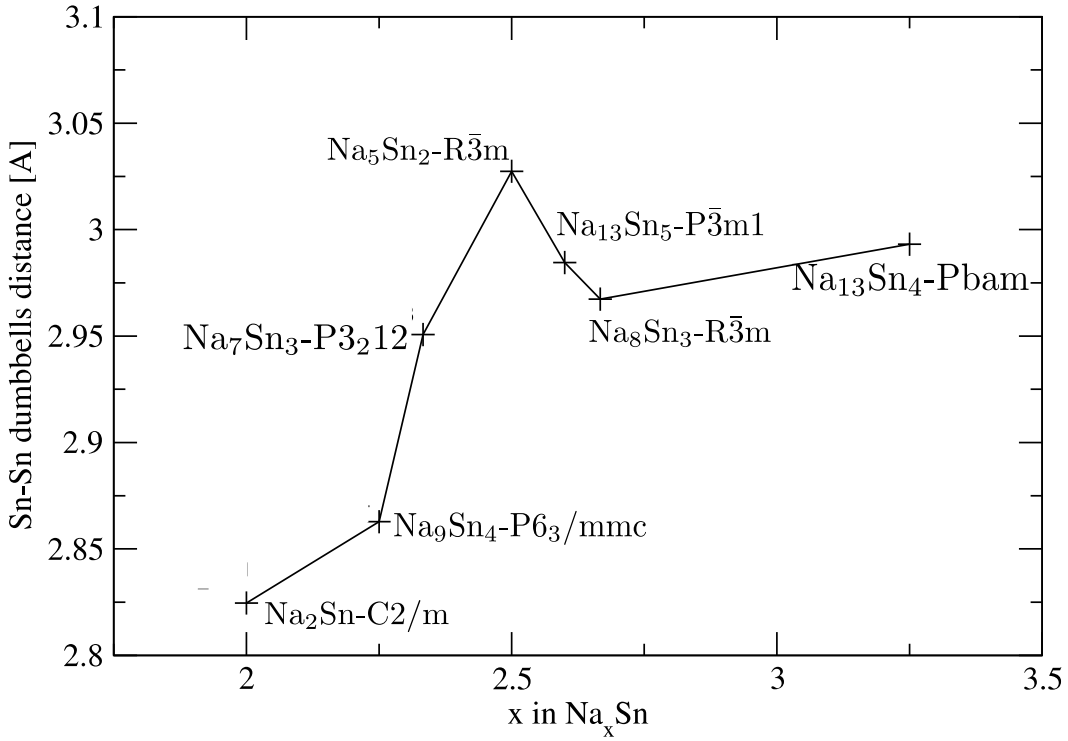

Figure S15. Sn-Sn dumbbell distances as a function of Na concentration.

***Ex situ* PDF and NMR data corresponding to the structures formed at the end of discharge**

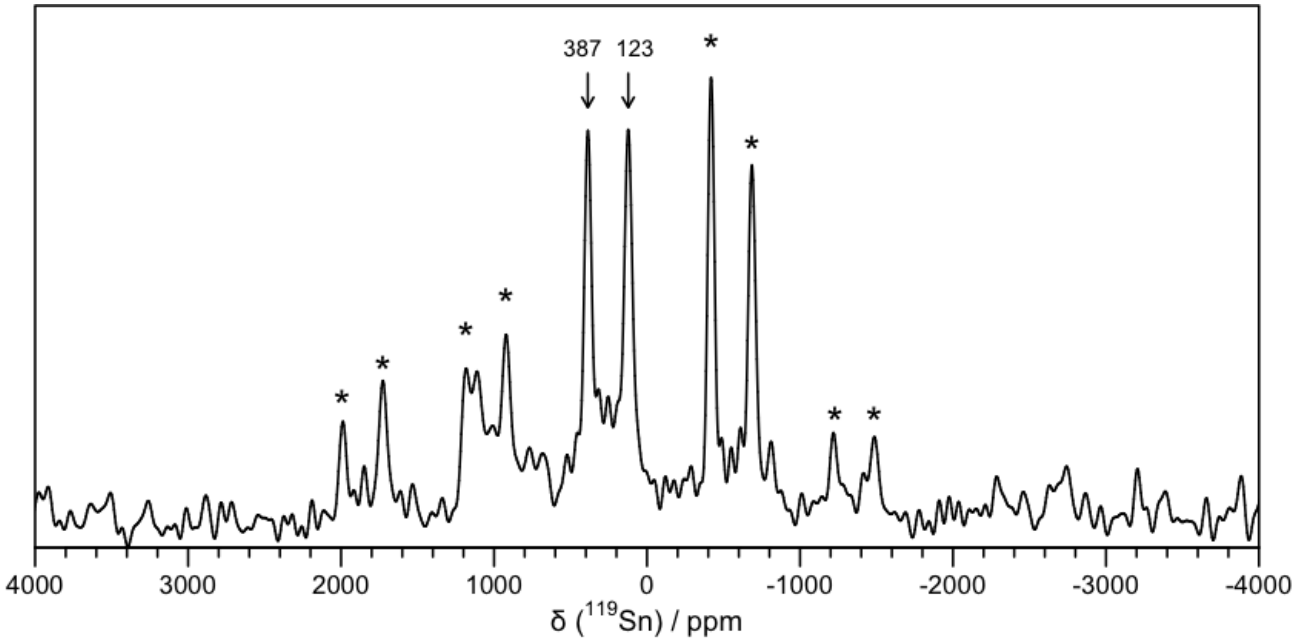

Figure S16. *Ex situ* ^{119}Sn 60 kHz MAS NMR spectra of a tin anode discharged to 1 mV. Shifts are indicated for isotropic peaks. A small, broad peak is also present around 1000 ppm, which corresponds to the structures formed during electrochemical processes 3 and 3′. Spinning sidebands are indicated with a *.

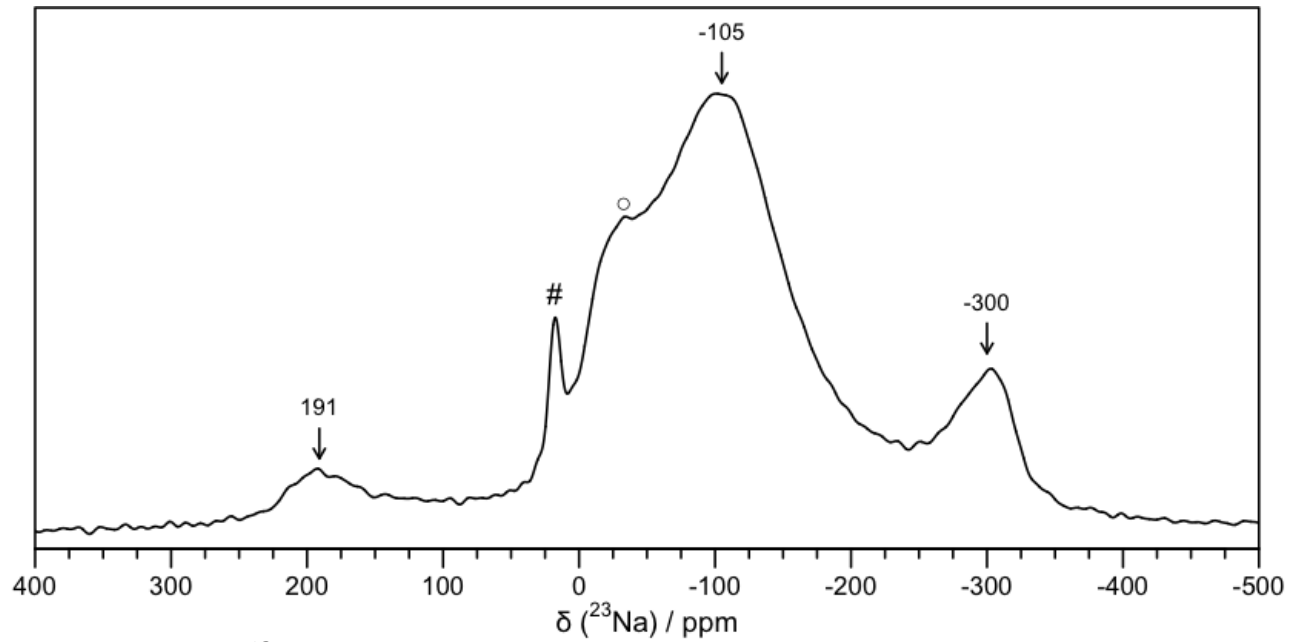

Figure S17. *Ex situ* ^{23}Na 60 kHz MAS NMR spectra of a tin anode discharged to 1 mV. Shifts are indicated for all peak maxima. The small, broad peak around 191 ppm corresponds to the structures formed during electrochemical processes 3 and 3′. The peak labelled # corresponds to trace amounts of NaOH, the peak labelled ○ results from sodium within the SEI layer, carbon additive and CMC binder.

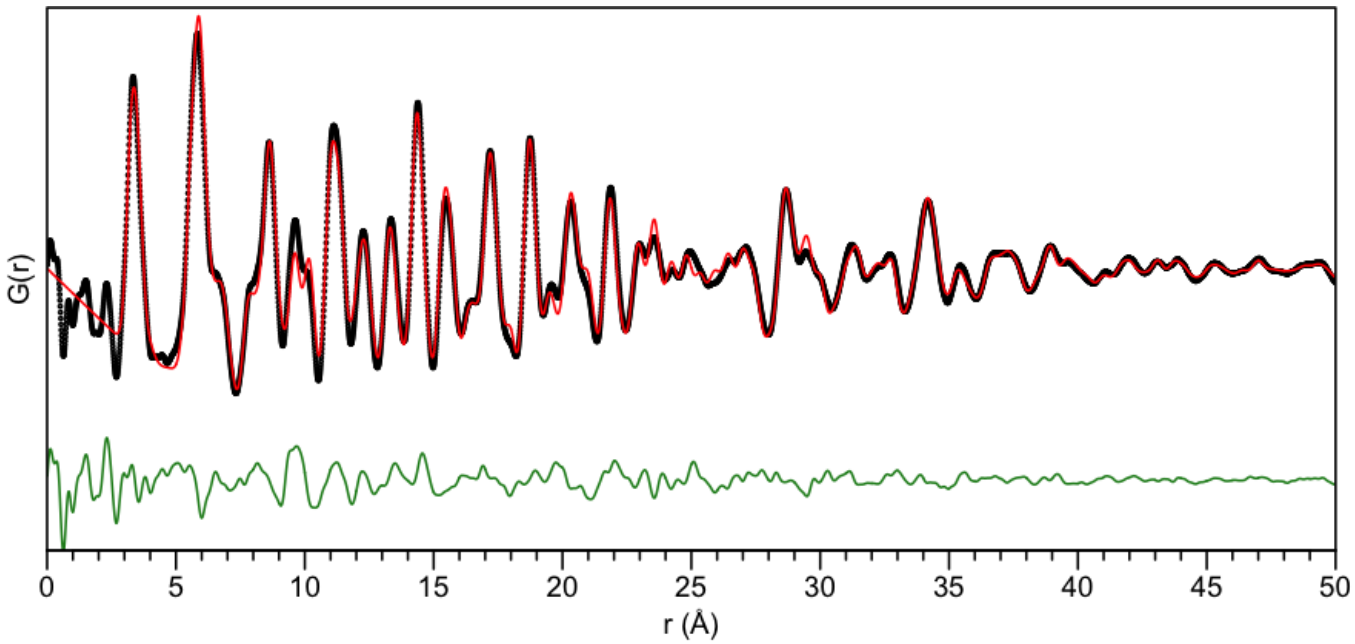

Figure S18. *Ex situ* PDF of a tin anode discharged to 1 mV. Experimental data are shown as black circles, a fit to $Na_{15}Sn_4$ (R_w=0.21) is shown as a red line and the difference as a green line offset below.

***In situ* ^{23}Na Measurements during relaxation of a discharged NaSn cell**

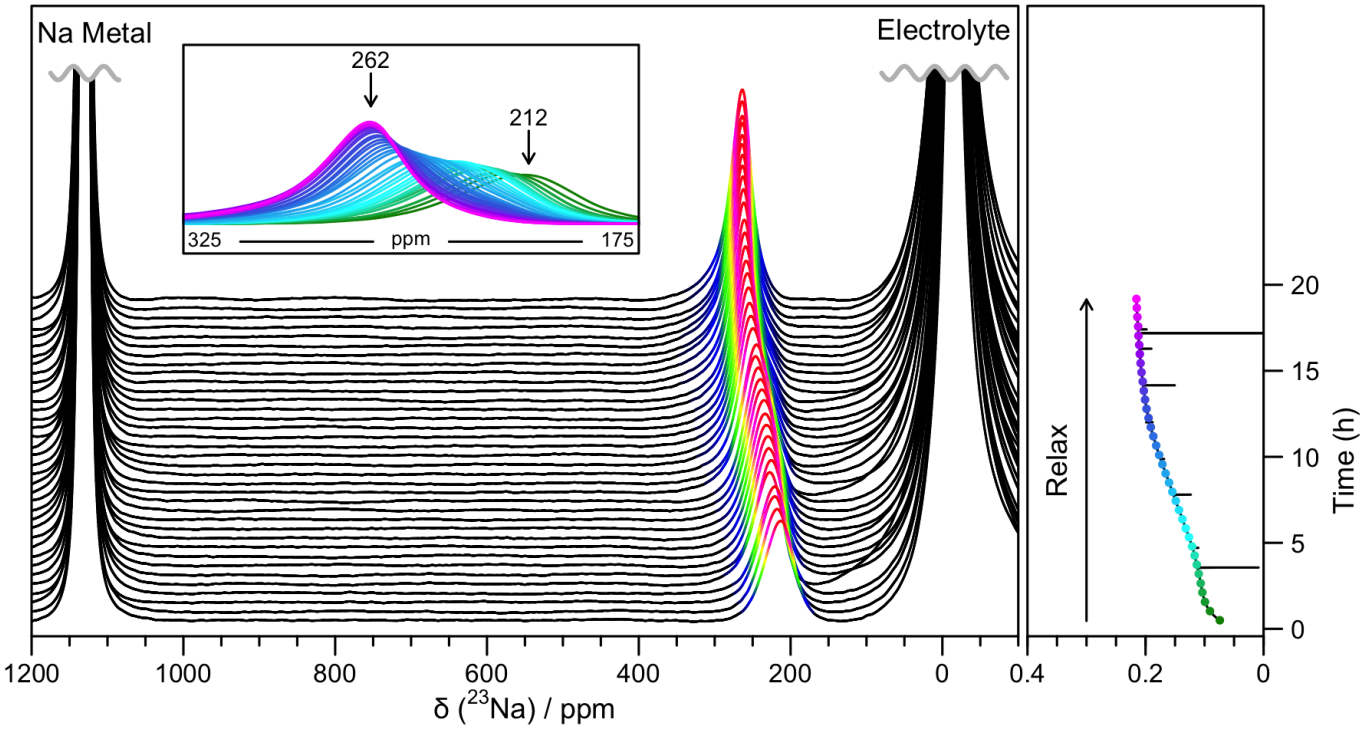

Figure S19. *In situ* ^{23}Na NMR measurement for a cell with sodium metal and tin electrodes, and a $NaPF_6$ electrolyte which was allowed to relax after discharging to the end of electrochemical process 3. NMR data is shown on the left, with the corresponding electrochemistry on the right. Strong features corresponding largely to the electrolyte or metal have been truncated for clarity. Spectra are coloured in the region 100–1000 ppm according to their intensity. Inset: a close-up of the region between 175-325 ppm highlighting the shifting peak. The colours now correspond to the points shown on the electrochemical curve.

Corresponding Electrochemistry *for operando* measurements

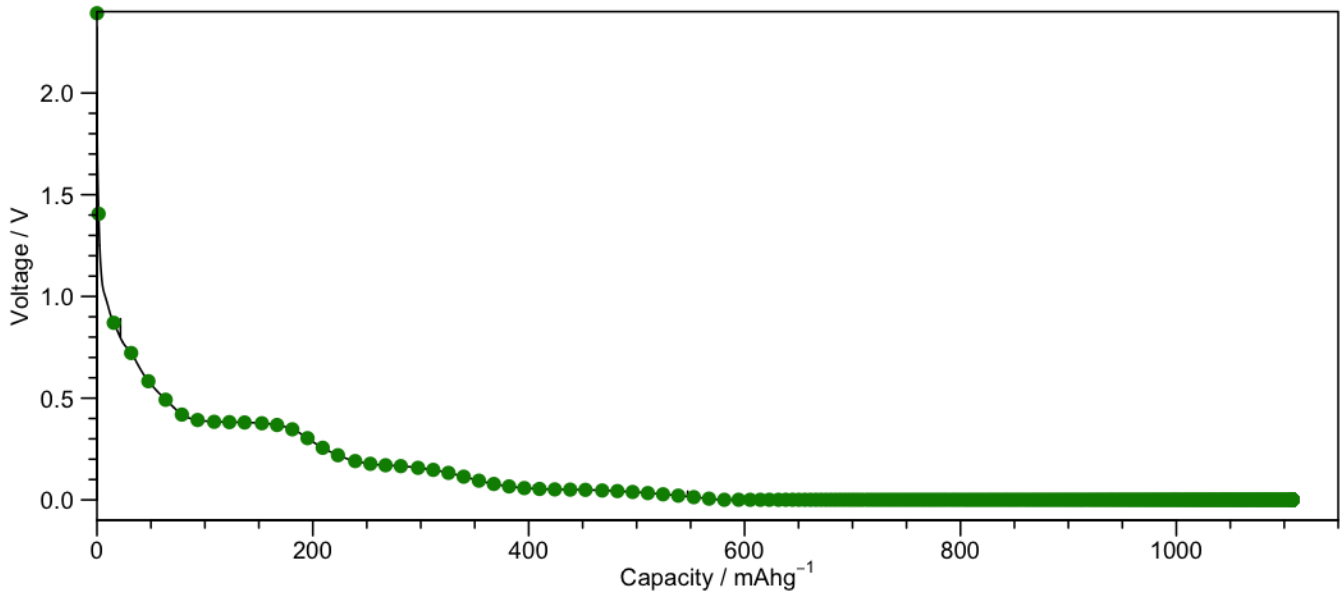

Figure S20. Corresponding electrochemistry data for the *operando* NMR measurement. The cell was cycled at a rate of C/30 (corresponding to achieving a capacity of 847 mAhg^{-1} in 30 hours) between 2 and 0.001 V (black line) and held at the end of discharge until the current dropped below C/100. Electrochemical data are shown as a black line, points at which NMR data were acquired are indicated with green circles.

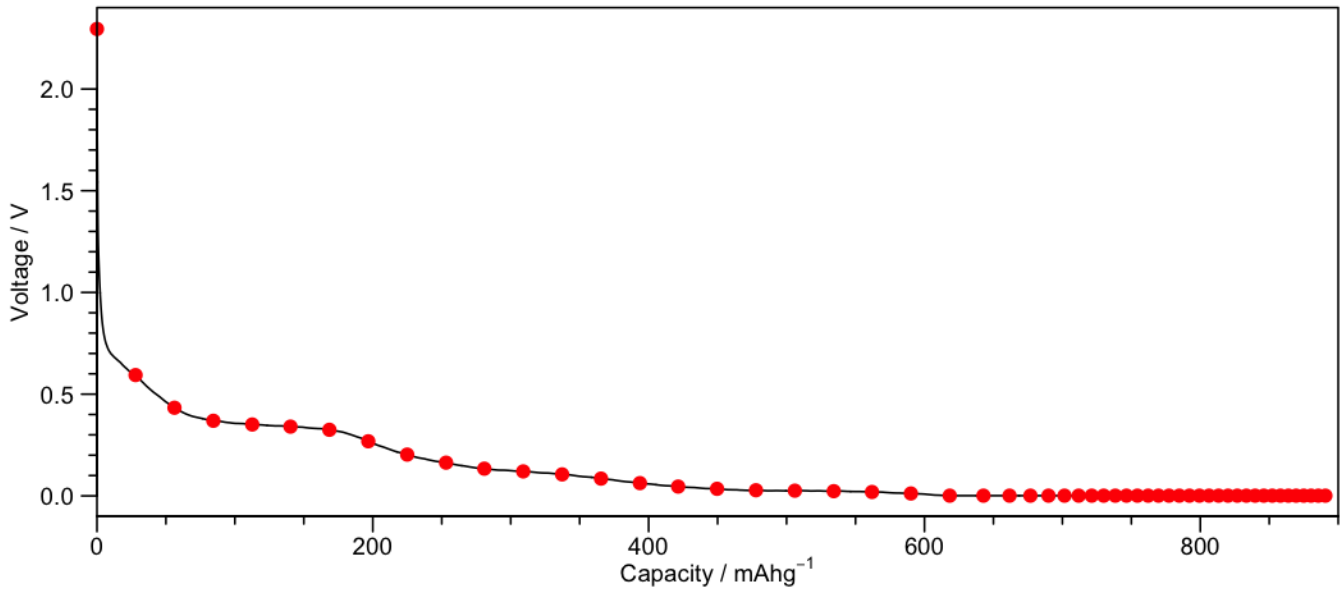

Figure S21. Corresponding electrochemistry data for the *operando* PDF measurement. The cell was cycled at a rate of C/30 (corresponding to achieving a capacity of 847 mAhg^{-1} in 30 hours) between 2 and 0.001 V (black line) and held at the end of discharge for the remainder of the beamtime. Electrochemical data are shown as a black line, points at which PDF data were acquired are indicated with red circles.

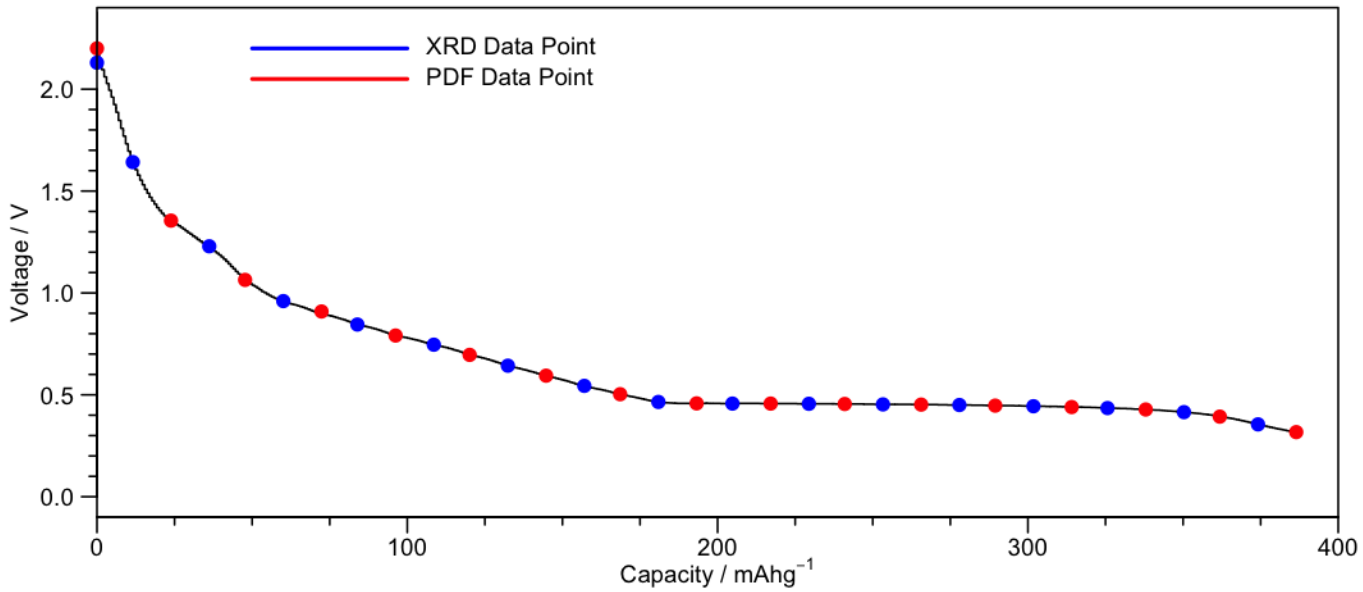

Figure S22. Corresponding electrochemistry data for the *operando* XRD and PDF measurement during processes 0, 1′ and 1. The cell was cycled at a rate of C/70 (corresponding to achieving a capacity of 847 mAhg^{-1} in 70 hours) between 2 and 0.32 V (black line). Electrochemical data are shown as a black line, points at which XRD, PDF data were acquired are indicated with blue, red circles.

Structural parameters for $NaSn_3$, $NaSn_2$ and Na_5Sn_2

Table S7. DFT calculated and experimentally refined lattice parameters for $NaSn_3$, $NaSn_2$ and Na_5Sn_2

	$NaSn_3$		$NaSn_2$		Na_5Sn_2	
	DFT*	Experiment	DFT	Experiment	DFT	Experiment†
Space Group	*Pmmm*		*P*6/*mmm*		*R*$\bar{3}$*m*	
a / Å	5.465	5.363	5.347	5.318	5.467	5.46
b / Å	9.292	9.224	–	–	–	–
c / Å	6.461	3.222	3.226	3.223	22.632	22.527
Na(1)	(0,0,0)	(0, 0, 0.5)	(0, 0, 0.5)		(0, 0, 0.21)	
Na(2)	(0,0,0.5)	(0.5, 0.5, 0.5)‡	–		(0, 0, 0.36)	
Na(3)	(0.5,0.5,0)	–	–		(0, 0, 0.5)	
Sn(1)	(0.5,0.83,0.25)	(0, 0.6667, 0)	(0.3333, 0.6667, 0)		–	
Sn(2)	(0,0.67,0.26)	(0.5, 0.1667, 0)	–		–	
Sn(3)	(0.5,0.5,0.5)	–	–		–	

* DFT structure corresponds to a 1×1×2 supercell of the experimental structure to remove partial occupancy

† Experimental structure has partial occupancies on site Na(3)

‡ Occupancy $Na_{0.5}Sn_{0.5}$

References

(1) Beekman, M.; Nenghabi, E. N.; Biswas, K.; Myles, C. W.; Baitinger, M.; Grin, Y.; Nolas, G. S. *Inorg. Chem.* **2010**, *49*, 5338–5340.
(2) Fässler, T. F.; Kronseder, C. *Angew. Chemie Int. Ed.* **1998**, *37*, 1571–1575.
(3) Fässler, T. F.; Hoffmann, S. *Inorg. Chem.* **2003**, *42*, 5474–5476.
(4) Müller, W.; Volk, K. *Z. Naturforsch. B* **1977**, *32*, 709–710.
(5) Axel, H.; Schäfer, H.; Weiss, A. *Angew. Chemie* **1965**, *77*, 379–380.
(6) Müller, W.; Volk, K. *Z. Naturforsch. B* **1978**, *33*, 275–278.
(7) Chevrier, V. L.; Zwanziger, J. W.; Dahn, J. R. *J. Alloys Compd.* **2010**, *496*, 25–36.
(8) Frank, U.; Müller, W.; Schäfer, H. *Z. Naturforsch. B* **1975**, *30*, 1–5.
(9) Frank, U.; Müller, W. *Z. Naturforsch. B* **1975**, *30*, 316–322.
(10) Zalkin, A.; Ramsey, W. J.; Templeton, D. H. *J. Phys. Chem.* **1956**, *60*, 1275–1277.
(11) Frank, U.; Müller, W.; Schäfer, H. *Z. Naturforsch. B* **1975**, *30*, 10–13.
(12) Müller, W.; Volk, K. *Z. Naturforsch. B* **1975**, *30*, 494–496.
(13) Goward, G. R.; Taylor, N. J.; Souza, D. C. S.; Nazar, L. F. *J. Alloys Compd.* **2001**, *329*, 82–91.
(14) Farrow, C. L.; Juhas, P.; Liu, J. W.; Bryndin, D.; Božin, E. S.; Bloch, J.; Proffen, T.; Billinge, S. J. L. *J. Phys. Condens. matter* **2007**, *19*, 335219.
(15) Tucker, M. G.; Keen, D. A.; Dove, M. T.; Goodwin, A. L.; Hui, Q. *J. Phys. Condens. Matter* **2007**, *19*, 335218.
(16) Baggetto, L.; Ganesh, P.; Meisner, R. P.; Unocic, R. R.; Jumas, J.-C.; Bridges, C. A.; Veith, G. M. *J. Power Sources* **2013**, *234*, 48–59.
(17) Shannon, R. D. *Acta Crystallogr. Sect. A* **1976**, *32*, 751–767.